

## Article

# Transport of Non-Steroidal Anti-Inflammatory Drugs across an Oral Mucosa Epithelium In Vitro Model

Grace C. Lin<sup>1</sup>, Heinz-Peter Friedl<sup>1</sup>, Sarah Grabner<sup>1</sup>, Anna Gerhartl<sup>1</sup> and Winfried Neuhaus<sup>1,2,3,\*</sup> 

<sup>1</sup> Competence Unit Molecular Diagnostics, AIT Austrian Institute of Technology GmbH, 1210 Vienna, Austria; anna.gerhartl@gmail.com (A.G.)

<sup>2</sup> Department of Medicine, Faculty of Medicine and Dentistry, Danube Private University, 3500 Krems, Austria

<sup>3</sup> Division of Pharmaceutical Technology and Biopharmaceutics, University of Vienna, 1090 Vienna, Austria

\* Correspondence: winfried.neuhaus@ait.ac.at

**Abstract:** Non-steroidal anti-inflammatory drugs (NSAIDs) are one of the most prescribed drugs to treat pain or fever. However, oral administration of NSAIDs is frequently associated with adverse effects due to their inhibitory effect on the constitutively expressed cyclooxygenase enzyme 1 (COX-1) in, for instance, the gastrointestinal tract. A systemic delivery, such as a buccal delivery, of NSAIDs would be beneficial and additionally has the advantage of a non-invasive administration route, especially favourable for children or the elderly. To investigate the transport of NSAIDs across the buccal mucosa and determine their potential for buccal therapeutic usage, celecoxib, diclofenac, ibuprofen and piroxicam were tested using an established oral mucosa Transwell® model based on human cell line TR146. Carboxyfluorescein and diazepam were applied as internal paracellular and transcellular marker molecule, respectively. Calculated permeability coefficients revealed a transport ranking of ibuprofen > piroxicam > diclofenac > celecoxib. Transporter protein inhibitor verapamil increased the permeability for ibuprofen, piroxicam and celecoxib, whereas probenecid increased the permeability for all tested NSAIDs. Furthermore, influence of local inflammation of the buccal mucosa on the transport of NSAIDs was mimicked by treating cells with a cytokine mixture of TNF- $\alpha$ , IL-1 $\beta$  and IFN- $\gamma$  followed by transport studies with ibuprofen (+ probenecid). Cellular response to pro-inflammatory stimuli was confirmed by upregulation of cytokine targets at the mRNA level, increased secreted cytokine levels and a significant decrease in the paracellular barrier. Permeability of ibuprofen was increased across cell layers treated with cytokines, while addition of probenecid increased permeability of ibuprofen in controls, but not across cell layers treated with cytokines. In summary, the suitability of the in vitro oral mucosa model to measure NSAID transport rankings was demonstrated, and the involvement of transporter proteins was confirmed; an inflammation model was established, and increased NSAID transport upon inflammation was measured.



**Citation:** Lin, G.C.; Friedl, H.-P.; Grabner, S.; Gerhartl, A.; Neuhaus, W. Transport of Non-Steroidal Anti-Inflammatory Drugs across an Oral Mucosa Epithelium In Vitro Model. *Pharmaceutics* **2024**, *16*, 543. <https://doi.org/10.3390/pharmaceutics16040543>

Academic Editors: Franciska Erdő, Heidi Kidron and Anna Sobańska

Received: 12 March 2024

Revised: 8 April 2024

Accepted: 10 April 2024

Published: 15 April 2024



**Copyright:** © 2024 by the authors. Licensee MDPI, Basel, Switzerland. This article is an open access article distributed under the terms and conditions of the Creative Commons Attribution (CC BY) license (<https://creativecommons.org/licenses/by/4.0/>).

**Keywords:** inflammation; TR146; blood–saliva barrier; non-steroidal antiphlogistic drugs

## 1. Introduction

The discovery of salicylic acid in the 19th century led to the formulation of one of the most popular drugs to treat inflammation and pain, acetylsalicylic acid, also known as aspirin [1]. Since then, several substances of various chemical structures with anti-inflammatory and antipyretic properties have been discovered and are classed as non-steroidal anti-inflammatory drugs (NSAIDs) [2]. NSAIDs have the advantage of lesser adverse side effects compared to other analgesics, such as opioids [3–5], and remain one of the most described drugs worldwide [6]. Their therapeutic effect is due to the inhibition on cyclooxygenase 1 and 2 (COX), of which COX-1 is constitutively expressed in the tissue (i.e., gastrointestinal tract) and described as a housekeeping gene, whereas COX-2 is upregulated upon inflammation [7]. The COX enzymes catalyse the conversion of arachidonic acid into thromboxane and prostaglandin, eicosanoids with pro-inflammatory

activities on the site of inflammation [8–11]. However, the functionality of prostaglandins are very versatile, as they also play a protective role in the gastrointestinal tract [10]. Hence, inhibition of COX-1 compromises the integrity of the gastrointestinal mucosa, leading to adverse effects such as gastrointestinal bleeding or stomach ulcers [12]. For this reason, NSAIDs are grouped into non-selective NSAIDs (ibuprofen, diclofenac, piroxicam) and COX-2 selective NSAID (celecoxib). Additionally, due to their diverse chemical structures, they are also grouped accordingly into salicylic acid derivatives (i.e., aspirin), propionic acid derivatives (i.e., ibuprofen, naproxen), acetic acid derivatives (i.e., indomethacin), enolic acids (i.e., piroxicam) or diaryl heterocyclic acids (i.e., celecoxib), among others [9,13,14]. Up to date the majority of NSAIDs on the market belong to the group of non-selective NSAIDs [9]. Additionally, COX-3, a splice variant of COX-1, expressed in the heart and cerebral cortex, has shown to be inhibited by paracetamol (more commonly known as acetaminophen) [15]. However, findings of COX-3 inhibition in humans are inconclusive [16].

With regard to the adverse effect on the gastrointestinal mucosa, circumventing the gastrointestinal tract and first-pass metabolism via systemic delivery of NSAIDs is beneficial, especially for patients requiring long-term treatment. While drugs are frequently administered via the intravenous route for this purpose, injections are often associated with discomfort and require trained personnel. Especially children are affected by fear of needles; however, adults have also been reported to delay medical treatments due to traumatic experiences with needles [17,18]. For these reasons, delivery by buccal absorption is preferable next to sublingual absorption, as the highly vascularised oral mucosa offers the possibility of non-invasive drug delivery while circumventing the gastrointestinal tract. In recent years, the suitability of biomaterials for regulated drug release has been studied intensively. Until now, several studies describing desirable composition and formulation of biomaterials (i.e., based on hydrogels or cellulose) for drug delivery have been published and summarised [19,20]. Recent studies with an NSAID as therapeutic agent describe buccal delivery systems for ibuprofen and indomethacin based on lipid nanoparticles loaded on mucoadhesive hydrogels and cellulose film [21,22]. To date, several buccal formulations with a wide range of drugs to treat insomnia or angina have been introduced to the market, including products based on opioids fentanyl and sufentanil for analgesic treatment [19]. However, marketed buccal formulations for pain treatment based on NSAIDs remain limited. Even though the buccal delivery route offers the advantage of bypassing the gastrointestinal tract, the effective absorption of drugs with low lipid solubility or larger molecular size is often limited and most drugs are assumed to cross the barrier using the paracellular or transcellular route by passive diffusion [23].

In this study, we aimed to investigate the permeability of NSAIDs of various chemical structures (acetic acid derivatives: diclofenac, propionic acid derivatives: ibuprofen, enolic acid derivatives: piroxicam) and selectivity (COX-2 selective: celecoxib) in more detail to evaluate their potential for buccal delivery. For this purpose, we used a thoroughly characterised model of the human buccal mucosa, which has been previously demonstrated to be suitable to study transport mechanisms of larger molecules [24,25]. Furthermore, we aimed to evaluate the influence of multidrug resistance transporter inhibitors probenecid and verapamil on the permeability of NSAIDs, as they have shown to increase the anti-inflammatory effect or transport of dauricine or NSAIDs in previous studies [26–28]. Additionally, we aimed to induce an inflammatory response by exposure to pro-inflammatory cytokines and assess the influence of the inflammation on the permeability of the selected NSAID ibuprofen.

## 2. Materials and Methods

### 2.1. Cell Culture

Human buccal carcinoma cells TR146 were purchased from Sigma-Aldrich (St. Louis, MO, USA), (10032305) and cultivated as described in detail previously [24]. In short, cells were cultivated in Dulbecco's Modified Eagle Medium (DMEM, Sigma-Aldrich, D5796) supplemented with 10% Fetal Calf Serum (Sigma-Aldrich, F9665) and 1% Peni-

cillin/Streptomycin (Merck, St. Louis, MO, USA, A2213) at 37 °C and propagated weekly at a cell density of  $9.33 \times 10^3/\text{cm}^2$ . For transport studies, cells were seeded at a density of  $4.29 \times 10^4/\text{cm}^2$  in cultivation media on 24-well ThinCerts (Greiner, Kremsmünster, Austria, 662641), and for Western blot analysis on 6-well ThinCerts (Greiner, 657641). As soon as cells reached confluency, cultivation was switched from submerged to airlift and 1% Human Keratinocytes Growth Supplements (HKGS, Gibco, ThermoFisher, Vienna, Austria, S0015) was added to the cultivation media on the basolateral compartment. Media were changed every 2–3 days until the day of experiment on day 29. Cells from passage 14–36 were used for experiments. Transepithelial electric resistance (TEER) was measured on day of experiment, as described in detail previously [25,29].

## 2.2. Transport Study

Piroxicam (P5654), ibuprofen (I1892) and probenecid (P8761) were purchased from Sigma-Aldrich, verapamil (94837) and carboxyfluorescein (21877) from Fluka, celecoxib, diclofenac and diazepam were a kind gift from Dr. Maierhofer (AGES, PharmMed, Vienna, Austria). Substances were dissolved in DMSO (Roth, Graz, Austria, A994.2), dd-H<sub>2</sub>O, or cultivation media for stock solutions (piroxicam: 100 mM in DMSO; carboxyfluorescein: 2.657 mM in cultivation media; celecoxib: 100 mM in DMSO; diclofenac: 3 mM in dd-H<sub>2</sub>O; ibuprofen: 10 mM in dd-H<sub>2</sub>O; diazepam: 100 mM in DMSO; probenecid: 100 mM in DMSO; verapamil; 100 mM in DMSO), sterile filtered and stored at 4 °C until usage. Solutions were diluted to 10 µM (carboxyfluorescein) or 100 µM in DMEM on day of experiments.

First, TEER was measured in cultivation media on the day of experiment. Afterwards, cells and blanks were washed twice with DMEM on the apical (300 µL) and basolateral (900 µL) compartments and selected cells and blanks were treated with DMEM with or without 100 µM probenecid or verapamil on the apical and basolateral side at 37 °C for 30 min. Prior to the start of the experiment, apical media were replaced with DMEM containing 100 µM diazepam, 10 µM carboxyfluorescein and 100 µM of NSAID (celecoxib, diclofenac, ibuprofen or piroxicam). To cells which were pre-incubated with probenecid or verapamil, 100 µM probenecid or verapamil was applied apically as well. DMSO content was adapted for cells with no inhibitors, and DMSO and dd-H<sub>2</sub>O content was adjusted in the basolateral compartment as well in order to apply the same vehicle concentrations on the apical and basolateral compartment. Cells were incubated in the dark at 37 °C, 5% CO<sub>2</sub> and 95% humidity, and every 60 min, cells and blank inserts were transferred to fresh basolateral media of the same composition. After 240 min, media from apical and basolateral compartments were collected for analysis and stored at 4 °C together with prepared stock solutions and media blanks. Samples were measured as duplicates (apical samples) or triplicates (basolateral samples, stock solutions, blank solutions) at 488/520 nm excitation/emission wavelength to estimate relative fluorescence units (RFU) of carboxyfluorescein using the Enspire Multimode Plate Reader (PerkinElmer, Traiskirchen, Austria). Subsequently, duplicates of apical sample were collected, and samples were frozen at –80 °C until further analysis with High-Performance Liquid Chromatography (HPLC).

## 2.3. High-Performance Liquid Chromatography

To analyse NSAIDs and diazepam, samples were thawed and precipitated with gradient-grade ( $\geq 99.9\%$ ) acetonitrile (CAN; VWR, Radnor, PA, USA, 83639.400, HiPerSolv Chromanorm<sup>®</sup>) in a one-part-plus-one-part ratio for at least 1 h at 4 °C. After centrifugation for 10 min at  $11,384 \times g$  rpm at 4 °C, supernatants were transferred to 1.5 mL transparent glass vials with 11 mm nominal diameter (Machery-Nagel, Vienna, Austria, 70201HP) and vials were sealed with 11 mm aluminium crimp closures (Machery-Nagel, 702001) using a manual crimper (Thermo Scientific, Vienna, Austria, 4012-100). ACN and 10 mM KH<sub>2</sub>PO<sub>4</sub> (Sigma-Aldrich, P0662-500G)—adjusted to pH 3 with 10 mM 85% H<sub>3</sub>PO<sub>4</sub> (Sigma-Aldrich, 49685-100 mL)—were degassed in an ultrasonic bath for at least 30 min prior to usage. Quantification was performed using an UltiMate<sup>™</sup> 3000-System (Thermo Fisher Scientific) equipped with HPG-3400SD standard binary pump (Thermo Fisher Scientific,

5040.0041), Dionex™ TCC-3200 column compartment (Thermo Fisher Scientific, 5730.0010), Dionex™ DAD-3000 variable wavelength detector (Thermo Fisher Scientific, 5082.0010) and WPS-3000TSL auto sampler (Thermo Fisher Scientific, 5822.0020). Sample injection volume was 10 µL and separated at a flow rate of 1 mL/min using a BDS Hypersil™ C18 column (Thermo-Fisher, 28105-254630, 250 × 4.6 mm, 5 µm particle size) equipped with a BDS Hypersil™ C18 5 µm 10 × 4 drop-in guard column (Thermo-Fisher, Vienna, Austria, 28105-014001).

Quantification of NSAID solutions with diazepam was performed with isocratic elution with different ratios of acetonitrile (ACN) and buffer (10 mM KH<sub>2</sub>PO<sub>4</sub>/10 mM H<sub>3</sub>PO<sub>4</sub>, pH = 3) except for celecoxib (diclofenac: 47:53 ACN/buffer; piroxicam 50:50 ACN/buffer, ibuprofen 60:40 ACN/buffer). To analyse solutions containing celecoxib and diazepam, diazepam was first detected at 11 min retention time after running with 45:55 ACN/buffer, then the ratio was increased to 80:20 ACN/buffer in a gradient from 12 to 14 min, then continued to run isocratically from 14 to 18 min with 80:20 ACN/buffer; celecoxib was detected at 18 min and ACN was reduced to 45% between 18 and 20 min run time. To reach equilibrium, the column was washed with 45:55 ACN/buffer from 20 to 22 min before the start of the next analysis run. Celecoxib, diclofenac and ibuprofen were detected at 220 nm, diazepam at 254 nm and piroxicam at 350 nm. NSAIDs with diazepam and verapamil were separated in the same manner as NSAIDs and diazepam. Solutions containing NSAIDs, diazepam and probenecid were separated with 35:65 ACN/buffer for 25 min, a gradient from 25 to 30 min to reach 80:20 ACN/buffer and running at 80:20 ACN/buffer from 30 to 34 min. Subsequently, a gradient was applied from 34 to 36 min to reach 35:65 ACN/buffer and the column was further equilibrated at 35:65 ACN/buffer from 36 to 38 min. Samples collected after transport studies, applied stock solutions and background media were measured in triplicates. Peaks were quantified using the software Chromeleon Version 7.2.6, and corresponding mili absorbance unit × time [mAU × min] values were used for data analysis.

#### 2.4. Calculation of Permeability Coefficient

Mean values of relative fluorescence unit (RFU) or detected area [mAU × min] were used for calculation. For the first timepoint, the clearance [µL] for the detected area was calculated as shown in the formula below (1a), with  $A_{baso_{t_1}}$  as the measured area [mAU × min] at the first time point of the basolateral sample,  $V_{baso}$  as the basolateral volume [µL] and  $A_{stock}$  as the area measured for the applied stock solution. For further time points, clearance was similarly calculated as in Formula 1b, subtracting summarised clearance of the previous time point multiplied by the volume factor for basolateral/apical of 3. Clearance [µL] for carboxyfluorescein was calculated with the same formulas using RFU.

$$Clearance = A_{baso_{t_1}} \times \frac{V_{baso}}{A_{stock}} \quad (1a)$$

$$Clearance_{t_n} = A_{baso_{t_n}} \times \frac{V_{baso}}{A_{stock} - \sum (A_{baso(t_{n-1})} \times 3 - A_{baso_{t_1}} \times 3)} \quad (1b)$$

Cleared volume [µL] was calculated by plotting the sum of clearance at all time points over time [min]. The resulting slope PS [µL/min] was calculated inversely. For calculation of the PS<sub>cell</sub>, the inverse PS blanks were subtracted, as shown below in Formula (2).

$$\frac{1}{PS_{cell}} = \frac{1}{PS_{all}} - \frac{1}{PS_{blank}} \quad (2)$$

The final permeability coefficient is calculated by dividing the inverse PS<sub>cell</sub> by the area of the ThinCerts (0.336 cm<sup>2</sup>) and multiplying by a conversion factor to give the permeability coefficient as µm/min.

### 2.5. Inflammation Study

ThinCerts<sup>®</sup> were seeded with cells as described above. Stock solutions of tumour necrosis factor  $\alpha$  (TNF- $\alpha$ , Sigma-Aldrich, H8916, 10  $\mu$ g), Interleukin-1 $\beta$  (IL-1 $\beta$ , PeproTech, 200-01B, 2  $\mu$ g) and Interferon- $\gamma$  (IFN- $\gamma$ , PeproTech, Vienna, Austria, 300-02, 20  $\mu$ g) were prepared with Dulbecco's Phosphate Buffered Saline (DPBS, Thermo-Fisher Scientific, Vienna, Austria, 14190094) containing 0.1% bovine serum albumin (BSA, Roth, Graz, Austria, 8076.2) at a concentration of 10  $\mu$ g/mL and stored at  $-20$  °C until usage. Three days before the experiments, cell layers and blanks were washed twice on the basolateral compartment with 900  $\mu$ L cultivation media (DMEM supplemented with 10% Fetal Calf Serum and 1% Penicillin/Streptomycin) to remove anti-inflammatory hydrocortisone residues (a component of media supplement HKGS) and were further cultivated in cultivation media. Solutions for the inflammation study were prepared on the day of experiment in DMEM containing 3% 0.1%BSA/DPBS and 3% sterilised dd-H<sub>2</sub>O (control), 100 ng/mL of TNF- $\alpha$ , IL-1 $\beta$  and IFN- $\gamma$  each in 3% 0.1%BSA/DPBS and 3% sterilised dd-H<sub>2</sub>O (INF), 100 ng/mL of TNF- $\alpha$ , IL-1 $\beta$  and IFN- $\gamma$  each in 3% 0.1%BSA/DPBS and 100  $\mu$ M ibuprofen (INF + Ibu) or 3% 0.1%BSA/DPBS and 100  $\mu$ M ibuprofen (Ibu).

Prior to treating cells with prepared DMEM solutions, TEER was measured in cultivation media DMEM supplemented with 1% Penicillin/Streptomycin and 10% Fetal Calf Serum. Subsequently, cell layers and blanks were washed with DMEM (without supplements) twice on the apical and basolateral compartment, followed by TEER measurements in DMEM. Media of cells were replaced with previously prepared DMEM solutions. Control media was applied on the blanks. After 48 h treatment at 37 °C, 5% CO<sub>2</sub> and 95% humidity TEER was measured. Subsequently, 10  $\mu$ M carboxyfluorescein was added to the apical DMEM solutions and incubated in the incubator at 37 °C for 2 h. Media were immediately collected and measured for the RFU content using the EnSpire as described above. Afterwards, media were stored at  $-20$  °C until further usage. Two cell-grown ThinCerts<sup>™</sup> of each treatment were pooled as one sample with 350  $\mu$ L lysis buffer supplemented with 1%  $\beta$ -mercaptoethanol and stored at  $-80$  °C for RNA isolation.

Transport studies with ibuprofen were performed directly after permeability studies with carboxyfluorescein. Selected cells and blanks were pre-incubated with DMEM containing 100  $\mu$ M probenecid for 30 min at 37 °C, as described above. Apical media were replaced with DMEM solutions containing 100  $\mu$ M ibuprofen, 100  $\mu$ M diazepam and 10  $\mu$ M carboxyfluorescein. Solutions for cells and blanks pre-incubated with probenecid additionally contained 100  $\mu$ M probenecid on the apical and basolateral compartment. Solutions for cells and blanks without prior probenecid treatment contained 1% sterile DMSO as vehicle instead. Transport studies were subsequently performed, as described above in Section 2.2.

### 2.6. Quantitative Real-Time PCR

Cell samples were lysed, and RNA was isolated and transcribed to cDNA synthesis, as described in detail previously [24]. In short, RNA of cell lysates was isolated using the NucleoSpin RNA kit (Machery Nagel, 740961) and 1  $\mu$ g RNA was transcribed in cDNA using the High-Capacity Reverse Transcriptase Kit (Applied Biosystems<sup>™</sup> Thermo Scientific, 4374967) synthesis. For qPCR, samples were analysed as triplicates using the LightCycler480 II (Roche) with the program described in Lin et al. [24] with primers for 18SrRNA (5'-3' forward: ATGGTTCCTTGGTCGCTCG, 5'-3' reverse: GAGCTCACCGGGTTGGTTTT), Janus Kinase 1 transcript variant a (JAK1tva) (5'-3' forward: TGACCGTCACCTGCTTTGAG, 5'-3' reverse: GGTTGGAGATTCTCGGGC), JAK1tvb (5'-3' forward: GGGATATTTCCCTGGCCTTCT, 5'-3' reverse: AAGAGATCCAGAGGACCCCC), JAK1tvc (5'-3' forward: CTTTGCCCTGTATGACGAGAAC, 5'-3' reverse: ACCTCATCCGGTAGTGAGC), TNF Receptor Associated Factor 2 (TRAF2) tvb (5'-3' forward: AAAGCAGTTCGGCCTTCCC, 5'-3' reverse: TCCTTTTACCAAGGCGGAC), TRAF2tvc (5'-3' forward: CCTTCCAGATAATGCTGCC, 5'-3' reverse: GCTCTCGTATTCTTTCAGGGTC) and nuclear factor  $\kappa$ B (NF- $\kappa$ B) RelA (forward 5'-3': ACTGTTCCCCCTCATCTTCC, reverse 5'-3': TG

GTCCTGTGTAGCCATTGA). Data were acquired with the LightCycler480 V1.5 software.  $\Delta$ Ct values were calculated by subtracting Ct values of 18SrRNA. Values were negatively exponentiated to the power of 2 and normalised to samples treated with inflammatory cytokines.

### 2.7. Western Blot

Cells seeded on 6-well ThinCerts for protein analysis were cultivated as described in the method in Section 2.1 using 2 mL media on the apical and 3.5 mL on the basolateral side. On day 29, cells were treated with DMEM containing 3% 0.1%BSA/DPBS plus 3% sterile dd-H<sub>2</sub>O (control), 100 ng/mL cytokines plus 3% sterile dd-H<sub>2</sub>O (INF), 100 ng/mL cytokines plus 100  $\mu$ M ibuprofen (INF+IBU) as well as 3% 0.1%BSA/DPBS plus 100  $\mu$ M ibuprofen (IBU) for 48 h, as described in the method in Section 2.5. Media were collected and stored at  $-20$  °C, while cell layers were washed twice with pre-cooled DPBS on ice. After 5 min incubation with DPBS after the last washing step, cells were lysed with 50  $\mu$ L RIPA buffer (50 mM TRIS pH 8.0; 150 mM NaCl, 0.1% SDS, 0.5% sodium-deoxycholate, 1% NP40), supplemented with complete ULTRA protease inhibitor cocktail and PhosphoSTOP minitab (Roche Applied Science, Penzberg, Germany, 288 05892970001 and 04906837001) for 30 min. Cell lysates were stored at  $-80$  °C and protein concentration was determined with the Pierce BCA assay kit (Thermo Fisher, Vienna, Austria, 23227) according to the manufacturer's instruction. Western blotting was performed as described previously [24]. In short, 20  $\mu$ g protein was loaded from each sample and primary antibody for COX-1 (Santa Cruz, Dallas, TX, USA, sc-19998, mouse) and COX-2 (Santa Cruz, sc-19999) was applied 1:200 and 1:200 in 5% non-fat dried milk (AppliChem Panreac, Darmstadt, Germany, A0830,0500). Subsequently, the HRP-labelled anti-mouse antibody was applied 1:5000 diluted in 5% non-fat dried milk (Cell signalling Technology, 7076S). For visualization of endogenous control  $\beta$ -actin, HRP-labeled  $\beta$ -actin antibody (Sigma-Aldrich, A3854, 7076S) was applied 1:20,000 in 5% non-fat dried milk. Signals were captured with Chemi-Doc Imaging system (BioRad, Hercules, CA, USA) and analysed with ImageLab Software Version 5.2.1.

### 2.8. Quantibody

Media samples from inflammation studies on 24-well inserts were collected at the end of the experiment after 48 h, stored at  $-20$  °C until analysis and thawed on ice on the day of quantification. Applied stock solution, apical and basolateral media from blanks and cells of all treatment conditions were used for measurements and diluted 1:2 in reagent diluent. Samples were processed according to the manufacturer's instructions of the Quantibody<sup>®</sup> Human Inflammation Array (Q1, QAH-INF-1-4, RayBiotech, Peachtree Corner, GA, USA) to quantify CCL2 (MCP1), CXCL8 (IL-8), INF- $\gamma$ , IL-10, IL-13, IL-1 $\alpha$ , IL-1 $\beta$ , IL-4, IL-6 and TNF $\alpha$ . Slides were recorded with an array scanner, images of the scanned arrays were processed by means of grid analysis and quantified with an xls-template from RayBiotech specified for the obtained array.

### 2.9. Statistical Analysis

Results are shown as mean  $\pm$  SD and mean  $\pm$  SEM when equipped for graphs with large sample sizes. Graphs were illustrated with SigmaPlot version 14.0 and statistical analysis was performed as one-way or two-way ANOVA with post hoc Holm-Sidak test and \*  $p < 0.05$ , \*\*  $p < 0.01$ , \*\*\*  $p < 0.001$  and  $\alpha = 0.05$  using SigmaPlot.

## 3. Results

### 3.1. Permeability of NSAIDs across the Oral Mucosa In Vitro

Figure 1A–D shows the cleared volume curves over time for the transport studies of NSAIDs and diazepam across blank and cell layer inserts. The black curves of the compounds across the blank inserts without cells indicate faster transport in comparison to the corresponding inserts with the cells, which confirmed that the oral mucosa barrier in vitro model formed a distinct barrier for the tested NSAIDs. In addition, it was recognizable that

the blank curves for diazepam and diclofenac, ibuprofen and piroxicam were very similar, underlining also very similar interactions of these compounds with the blank membranes. Notably, lower amounts of celecoxib already permeated across the blank inserts than for diazepam, indicating more interaction of celecoxib with the membrane and highlighting the importance of blank studies across only the membranes for each compound in order to account for these differences when assessing permeability coefficients. The white cleared volume curves over time suggested that diazepam permeated faster than every NSAID, which was expected for the transcellular marker diazepam. Notably, the paracellular marker substance carboxyfluorescein (CF) showed the highest clearance across blanks and cells of all substances applied (Figure 1E).

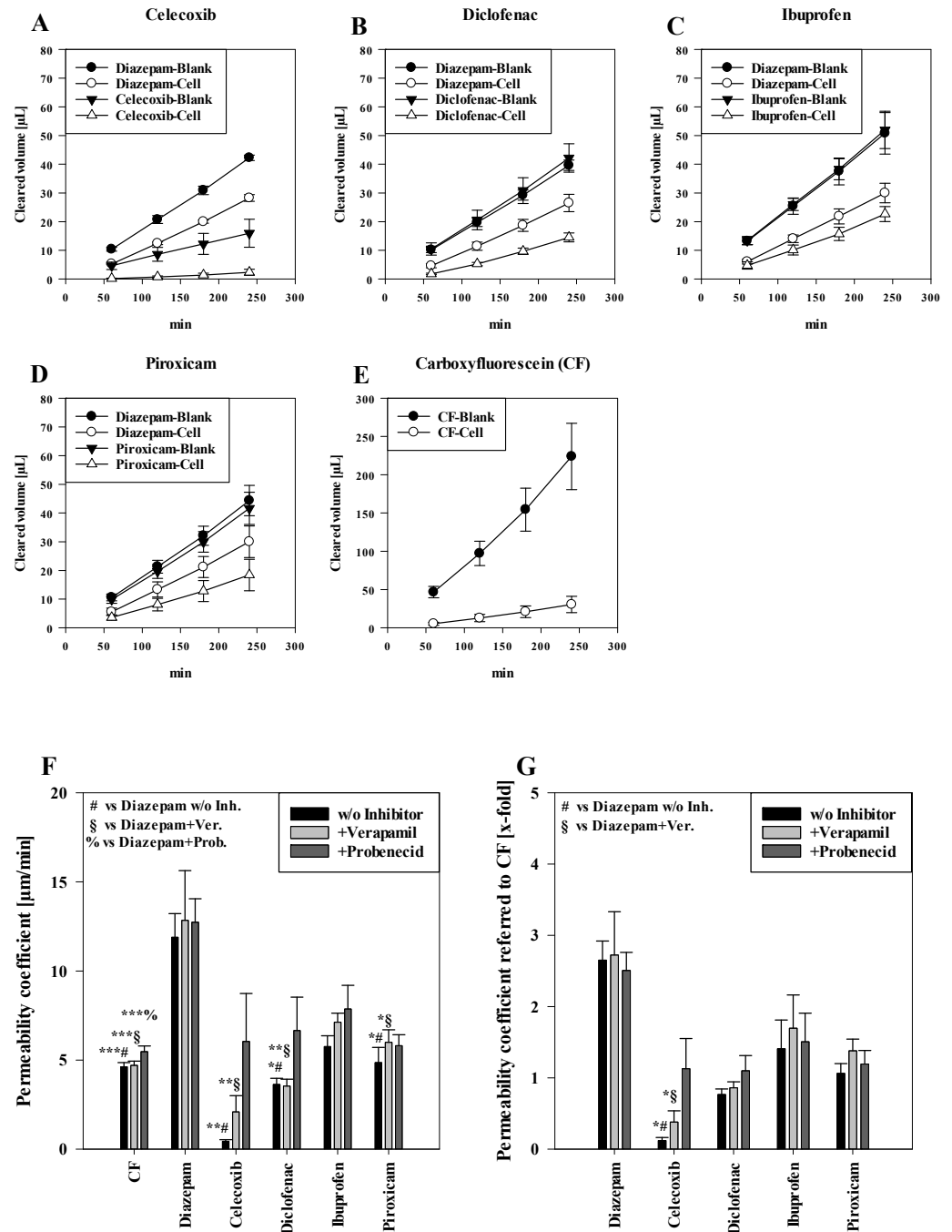


**Figure 1.** Measured cleared volume [μL] from blanks and cells over time [min] of (A) celecoxib, (B) diclofenac, (C) ibuprofen and (D) piroxicam with corresponding diazepam values from experiments.

Representative values for carboxyfluorescein (CF) measured in the piroxicam study shown in (E). Results shown as mean  $\pm$  SD from three independent experiments ( $n = 4-8$ ). Permeability coefficient of carboxyfluorescein, diazepam and NSAIDs without inhibitors and upon treatment with verapamil and probenecid shown as  $\mu\text{m}/\text{min}$  (F) and normalised to the respective permeability coefficient of CF (G). Results shown as mean  $\pm$  SEM from three independent experiments ( $n = 4-28$ ). Statistical analysis performed as two-way ANOVA with post hoc Holm-Sidak test, \*  $p < 0.05$ , \*\*  $p < 0.01$ , \*\*\*  $p < 0.001$  and  $\alpha = 0.05$ .

Corresponding to the cleared volume curves, the calculated permeability coefficients of paracellular marker CF ( $4.63 \pm 0.24 \mu\text{m}/\text{min}$ ,  $p < 0.001$ ) were significantly lower than for the transcellular marker diazepam ( $11.90 \pm 1.33 \mu\text{m}/\text{min}$ ) (Figure 1F). For applied NSAIDs, ibuprofen showed the highest permeability coefficient ( $5.77 \pm 0.60 \mu\text{m}/\text{min}$ , not significant (n.s.) compared to diazepam), followed by piroxicam ( $4.86 \pm 0.84 \mu\text{m}/\text{min}$ ,  $p < 0.05$ ) and diclofenac ( $3.64 \pm 0.34 \mu\text{m}/\text{min}$ ,  $p < 0.05$ ). Of all NSAIDs, celecoxib showed the lowest permeability coefficient ( $0.44 \pm 0.10 \mu\text{m}/\text{min}$ ,  $p < 0.01$ ). However, upon addition of verapamil or probenecid, celecoxib displayed the highest increase of 4.72-fold ( $2.10 \pm 0.92 \mu\text{m}/\text{min}$ ,  $p < 0.01$  vs. diazepam+verapamil) with verapamil and a 13.63-fold ( $12.74 \pm 1.31 \mu\text{m}/\text{min}$ , n.s.) increase with probenecid. On the other hand, the permeability coefficient of diclofenac did not change after verapamil treatment ( $3.54 \pm 0.38 \mu\text{m}/\text{min}$ ,  $p < 0.01$  vs. diazepam+verapamil.), while the addition of probenecid led to a 1.83-fold higher permeability coefficient ( $6.66 \pm 1.87 \mu\text{m}/\text{min}$ , n.s.). For ibuprofen and piroxicam, the addition of verapamil showed a slight increase of 1.23-fold for both NSAIDs (ibuprofen:  $7.13 \pm 0.51 \mu\text{m}/\text{min}$ , n.s.; piroxicam:  $6.00 \pm 0.70 \mu\text{m}/\text{min}$ ,  $p < 0.05$  vs. diazepam + verapamil) compared to no inhibitor. On the other hand, added probenecid led to a 1.36-fold increase in ibuprofen permeation ( $7.87 \pm 1.32 \mu\text{m}/\text{min}$ , n.s.) and to a 1.19-fold increase in the permeability coefficient of piroxicam ( $5.81 \pm 0.61 \mu\text{m}/\text{min}$ , n.s.).

As additional analysis, permeability coefficients of NSAIDs and diazepam were normalised to corresponding permeability coefficients of paracellular marker CF, shown in Figure 1E. As a result, diazepam showed very similar permeability coefficients regardless of the treatments (control: 2.65 ( $\pm 0.27$ )-fold, added verapamil: 2.72 ( $\pm 0.61$ )-fold, added probenecid: 2.51 ( $\pm 0.25$ )-fold in comparison to CF). Similarly as described above, celecoxib showed the lowest permeability coefficient (0.12  $\pm$  0.04-fold,  $p < 0.05$  vs. diazepam), which was increased by verapamil (0.38  $\pm$  0.15-fold,  $p < 0.05$  vs. diazepam + verapamil) and probenecid (1.29  $\pm$  0.42-fold) treatments, followed by diclofenac (0.77  $\pm$  0.08-fold, +verapamil: 0.86  $\pm$  0.08-fold, +probenecid: 1.10  $\pm$  0.21-fold). Similarly, ibuprofen showed the highest permeability (1.41  $\pm$  0.40-fold) of all NSAIDs, increased by verapamil (1.70  $\pm$  0.46-fold) and probenecid (1.51  $\pm$  0.40-fold) addition. Piroxicam displayed a permeability coefficient of 1.06  $\pm$  0.14-fold without inhibitors, and a permeability coefficient of 1.38  $\pm$  0.16 after addition of verapamil and 1.20  $\pm$  0.19-fold under probenecid (an overview of calculated slope values for calculation of the permeability of cells and blanks with corresponding TEER values is shown in Table S1).

### 3.2. Cytokines Induce Inflammatory Response in the Oral Mucosa Epithelium In Vitro Model

NSAIDs are very often applied during diseases to suppress inflammatory processes. It is known that inflammation can change the functionality of biological barriers, in particular transporter proteins as well as tight junctions determining the transcellular as well as the paracellular route of compounds. As a next step, we wanted to know whether the transport of NSAIDs would be changed under inflammatory conditions. Before conducting transport studies with NSAIDs across our inflamed oral mucosa in vitro model, we assessed effects of the applied cytokine mixture on our model to confirm that the stimuli induced inflammatory changes on the mRNA and the protein level. For these studies, we decided to investigate the effects of ibuprofen, because ibuprofen belongs to the most frequently used NSAIDs in Europe, Asia and Australia next to diclofenac [30,31], and ibuprofen has a bigger potential for future use, since a prevalence for stroke was found for diclofenac but not for ibuprofen [32]. First, we analysed the expression of JAK1, TRAF2 and RELA at

the mRNA level by qPCR after cytokine treatments. All transcript variants of JAK1 and TRAF2 were upregulated after cytokine addition in comparison to control cells as well as cells treated with ibuprofen only, but the addition of ibuprofen during inflammation did not block the upregulation of JAK1 and TRAF2 (Figure 2A). In the case of RELA, ibuprofen was also able to inhibit the increase in RELA by inflammatory cytokines in a significant manner ( $p < 0.05$ ), confirming the anti-inflammatory properties of ibuprofen in our model.

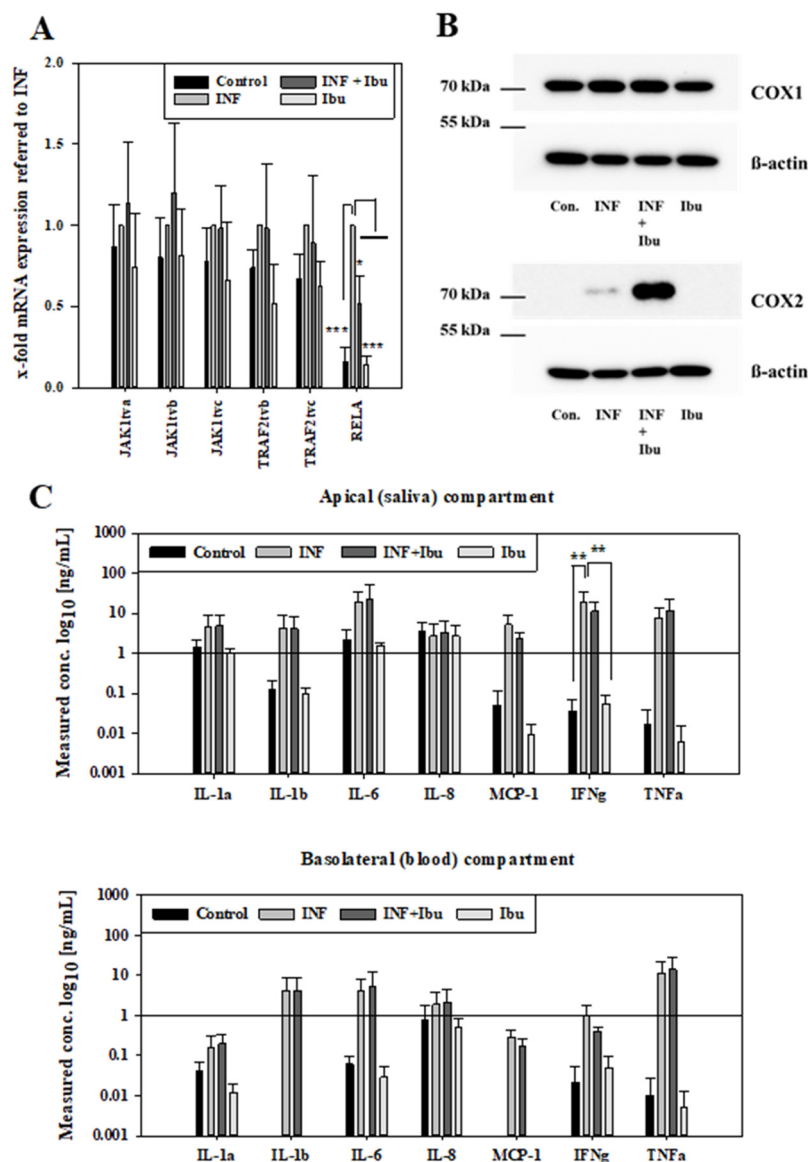


**Figure 2.** Samples from 48 h inflammation studies (control: media, INF: 100 ng/mL IL-1 $\beta$ , IFN- $\gamma$  and TNF- $\alpha$ , INF+Ibu: 100 ng/mL IL-1 $\beta$ , IFN- $\gamma$ , TNF- $\alpha$  and 100  $\mu$ M ibuprofen, Ibu: 100  $\mu$ M ibuprofen) analysed for mRNA expression of JAK1, TRAF2 and RELA. (A) Expression values referred to housekeeping gene 18SrRNA and shown normalised to samples treated with INF as mean  $\pm$  SD from three independent experiments. Statistical analysis performed as two-way ANOVA with post hoc Holm–Sidak test, \*  $p < 0.05$ , \*\*\*  $p < 0.001$ ,  $\alpha = 0.05$ . (B) Representative Western blot for COX-1 (70 kDa), COX-2 (70–72 kDa) and  $\beta$ -actin (42 kDa) after inflammation studies. (C) Measured concentration of cytokines in media from inflammation studies on the apical (saliva) and basolateral (blood) compartment. Results shown as mean  $\pm$  SD from three independent experiments. Statistical analysis performed as two-way ANOVA with post hoc Holm–Sidak test, \*\*  $p < 0.01$  and  $\alpha = 0.05$ .

At the protein level, the expression of COX-1 and COX-2 was verified by Western blotting using samples of inflammation studies. While all treatment groups showed a

similar expression of COX-1, an increased expression of COX-2 was observed for samples treated with cytokines or cytokines plus ibuprofen (Figure 2B). Moreover, it was tested whether the inflammatory stimuli also led to the secretion of cytokines. Concentrations of cytokines were measured in media of the apical (saliva) and basolateral (blood) compartments after cytokine mixture treatment. In the apical media, higher levels of IL-1  $\alpha$ , IL-1 $\beta$ , IL-6, MCP-1 and TNF- $\alpha$  were detected for samples treated with cytokines or cytokines with ibuprofen. IFN- $\gamma$  levels of samples treated with cytokines were significantly higher ( $p < 0.01$ ) compared to samples treated with ibuprofen or control samples. No regulation was observed for IL-8 among the treatment groups. In media from the basolateral compartment, higher levels of IL-1  $\alpha$ , IL-1 $\beta$ , IL-6, MCP-1, IFN- $\gamma$  and TNF- $\alpha$  were observed in samples treated with cytokines or cytokines and ibuprofen, while lower or no levels were observed for control samples or samples treated with ibuprofen. IL-4, IL-10 and IL-13 were not detected with the applied Quantibody<sup>®</sup> array after 48 h stimulation. In summary, inflammation of the oral mucosa epithelium in vitro model was confirmed at the mRNA and protein level by increase in respective marker molecules and the secretion of cytokines. After the inflammation protocol for the model was successfully established, the effects of the inflammation on transport routes were investigated.

### 3.3. Affected Transport Routes after Treatment with Pro-Inflammatory Cytokines

First, it was tested whether the inflammation affected the paracellular barrier integrity of the model. For this, transepithelial electrical resistance (TEER) was measured at the start of the experiment and after treatment with cytokines. Due to reproducibility reasons, the threshold for cell layers to be included into the study was set to a minimum TEER value of at least  $100 \Omega \times \text{cm}^2$ . TEER values at start and after 48 h are shown in Figure 3A. While control cells and cells treated with ibuprofen showed similar TEER values after 48 h ( $77.10 \pm 15.25 \Omega \times \text{cm}^2$ ,  $69.65 \pm 9.10 \Omega \times \text{cm}^2$ ), treatment with cytokines or cytokines plus ibuprofen displayed significantly lower ( $p < 0.001$ ) TEER values of  $45.30 \pm 5.10 \Omega \times \text{cm}^2$  and  $49.16 \pm 14.51 \Omega \times \text{cm}^2$ , respectively. Permeability assays performed with CF for two hours after 48 h inflammation treatment revealed a lower permeability coefficient for CF across control cells ( $12.41 \pm 5.15 \mu\text{m}/\text{min}$ ) and cells treated with ibuprofen ( $12.83 \pm 3.57 \mu\text{m}/\text{min}$ ) in comparison to cells treated with cytokines ( $16.16 \pm 13.05 \mu\text{m}/\text{min}$ ) or cytokines with ibuprofen ( $16.75 \pm 9.76 \mu\text{m}/\text{min}$ ), shown in Figure 3B. Thus, CF permeability data confirmed TEER data that inflammatory stimuli reduced the model's paracellular tightness and that the addition of ibuprofen did not block the cytokine-induced barrier breakdown.

To evaluate the effects of inflammation on transcellular transport routes, transport studies with ibuprofen plus probenecid were carried out. Ibuprofen and probenecid were chosen, since previous studies showed that ibuprofen was a substrate of transporters whose activity was inhibitable by probenecid [33]. As described above, CF and diazepam were added as control compounds during transport studies and permeability coefficients were calculated, drawing samples every 60 min for 4 h. For control cells and cells treated with ibuprofen, permeability coefficients of CF were quite similar (control:  $14.26 \pm 7.14 \mu\text{m}/\text{min}$ , plus ibuprofen:  $14.39 \pm 3.12 \mu\text{m}/\text{min}$ ), whereas exposure to the cytokine cocktail with and without ibuprofen led to an increased permeability of CF (cytokine:  $24.30 \pm 4.82 \mu\text{m}/\text{min}$ , cytokine + ibuprofen:  $25.04 \pm 6.73 \mu\text{m}/\text{min}$ ). This cytokine treatment dependency was also observed for permeability coefficients of ibuprofen, as the pre-treatment with cytokines or cytokines plus ibuprofen led to higher permeability coefficients (cytokine:  $20.01 \pm 12.92 \mu\text{m}/\text{min}$ ; cytokine + ibuprofen  $21.06 \pm 14.25 \mu\text{m}/\text{min}$ ) than across control cell layers ( $14.38 \pm 7.25 \mu\text{m}/\text{min}$ ) or cell layers treated with ibuprofen alone ( $11.55 \pm 1.23 \mu\text{m}/\text{min}$ ).

The addition of probenecid showed the tendency to decrease permeability coefficients of CF. For control cell layers and cell layers treated with ibuprofen, a reduction of 14.36% and 24.59% (not significant) was measured, while for cells treated with cytokines or cytokines and ibuprofen, a reduction of 25.03% and 18.90% was observed (not significant). On

the contrary, the addition of probenecid showed the tendency of an increased permeability of ibuprofen. In the control group, the addition of probenecid led to a 42.46% higher permeability of ibuprofen ( $p < 0.001$  vs. diazepam) and a 52.64% (not significant) higher permeability for cells treated with ibuprofen previously. However, cells treated with cytokines showed no distinct regulation of ibuprofen permeability with or without probenecid. In summary, inflammation increased permeation of CF and ibuprofen, which was probably due to a significantly decreased paracellular tightness. Interestingly, the addition of probenecid did not increase CF permeability, but enhanced ibuprofen permeability only across non-inflamed cell layers in the same experimental setting. This indicated that the probenecid-inhibitable part of ibuprofen transport was already affected after inflammation and that ibuprofen transport could not further be increased.

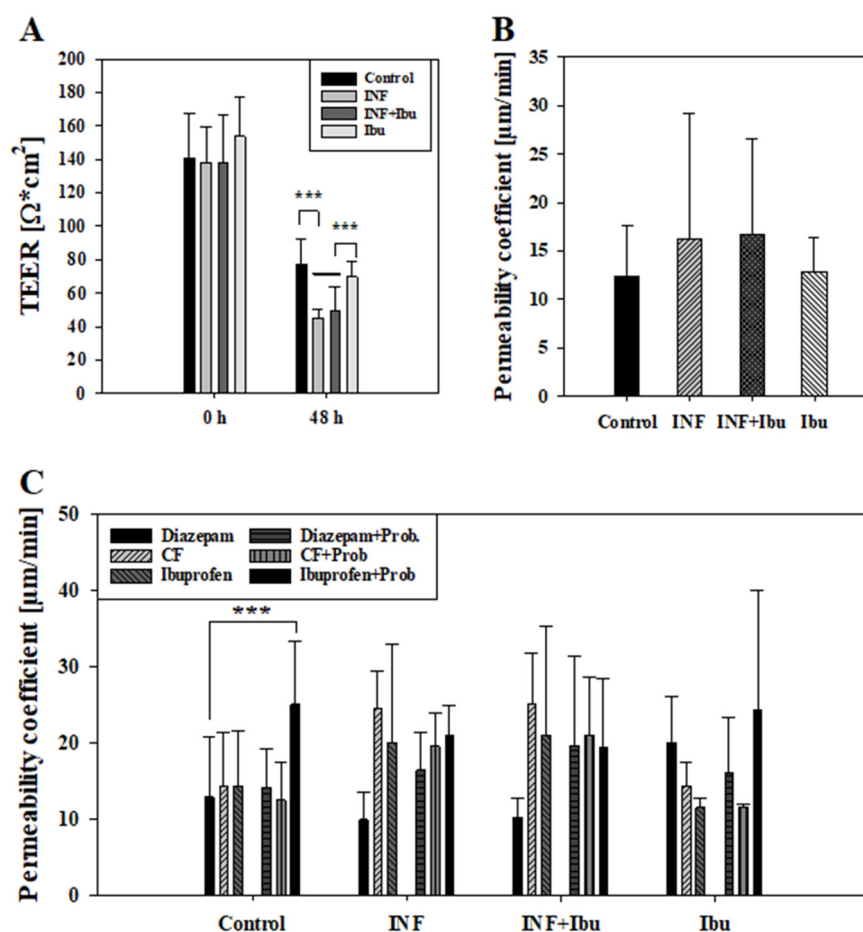


**Figure 3.** Measured TEER values [ $\Omega \times \text{cm}^2$ ] at start (0 h) and end (48 h) of experiment from control cells, cells treated with cytokines (INF), cytokines and 100  $\mu\text{M}$  ibuprofen (INF + Ibu) and 100  $\mu\text{M}$  Ibuprofen (Ibu) (A). Cells showing TEER values lower than 100  $\Omega \cdot \text{cm}^2$  at beginning of experiment were excluded from further data analysis. Results shown as mean  $\pm$  SD from three independent experiments ( $n = 13$ –17). Statistical analysis performed as one-way ANOVA following post hoc Holm–Sidak test with \*\*\*  $p < 0.001$  and  $\alpha = 0.05$ . (B) Corresponding permeability coefficient values of permeability assays with carboxyfluorescein performed at end of experiment (48 h). Results shown as mean  $\pm$  SD from three independent experiments ( $n = 13$ –17). Statistical analysis performed as one-way ANOVA with  $\alpha = 0.05$ . (C) Measured permeability coefficient from transport studies with diazepam, ibuprofen and carboxyfluorescein (CF) with and without probenecid (Prob) performed after 48 h. Results shown as mean  $\pm$  SD from three independent experiments ( $n = 3$ –6). Statistical analysis performed as two-way ANOVA following post hoc Holm–Sidak test with \*\*\*  $p < 0.001$  and  $\alpha = 0.05$ .

#### 4. Discussion

Even though up-to date NSAIDs are commonly prescribed orally, buccal delivery offers the major advantage of by-passing the gastrointestinal tract. The latter limits the adverse side effects caused by long-term usage of NSAIDs, such as gastric erosions or ulcers. Recently, technical advances were made to optimise buccal formulations for NSAIDs. For instance, Shirvan et al. (2021) developed a patch with potential for therapeutic usage by electrospinning of chitosan, polyvinylalcohol and ibuprofen and Eleftheriadis et al. (2020) described a printing technique with ibuprofen for personalised mucoadhesive films [34,35]. While an optimised formulation of patches or films is crucial to ascertain the delivery of drugs of interest at therapeutic concentrations, a thorough understanding of the transport mechanism of drugs of interest is essential to improve their buccal delivery.

For this purpose, we investigated the buccal transport of NSAIDs, using an established multi-layered model of the buccal mucosa to determine the permeability of celecoxib, diclofenac, ibuprofen and piroxicam. Diazepam, a standard for the transcellular transport route, was used for comparison [33]. Of applied NSAIDs, ibuprofen showed the highest permeability, followed by piroxicam, diclofenac and celecoxib (Figure 1F). Corresponding to this, literature data of a monolayer epithelial model of the humane intestine (Caco-2) showed the same ranking for NSAIDs, demonstrating the highest permeability for ibuprofen, followed by piroxicam [36], diclofenac and celecoxib [37,38]. In contrast, transport studies with monolayer brain endothelial models based on porcine (PBMEC/C1-2) and human (ECV304) cell lines showed the highest permeability for piroxicam, followed by ibuprofen, celecoxib and diclofenac for PBMEC/C1-2 or celecoxib and diclofenac for ECV304 [33]. Nevertheless, similar to our model, diazepam showed a higher permeation rate than NSAIDs in all three models (Caco-2, PBMEC/C1-2 and ECV304) [33,36]. Interestingly, the permeability coefficients of paracellular marker carboxyfluorescein (CF) across ECV304 cell monolayers were very similar compared to our model ( $\sim 5 \mu\text{m}/\text{min}$ ), while the permeability coefficients for the transcellular marker diazepam were distinctly higher across the ECV304 model ( $\sim 20\text{--}40 \mu\text{m}/\text{min}$ ) than in our model ( $\sim 12 \mu\text{m}/\text{min}$ ), reflecting the influence of multilayers (as in our buccal epithelium model) on the permeation of substances such as diazepam [33].

In accordance with the permeability coefficient, after four hours, the highest cumulated concentration of NSAID in the basolateral compartment was found for ibuprofen ( $0.067 \pm 0.0078 \text{ nmol}/\text{mm}^2$ , mean  $\pm$  SD,  $n = 6$ ), followed by piroxicam ( $0.055 \pm 0.016 \text{ nmol}/\text{mm}^2$ , mean  $\pm$  SD,  $n = 8$ ), diclofenac ( $0.043 \pm 0.0046 \text{ nmol}/\text{mm}^2$ , mean  $\pm$  SD,  $n = 6$ ) and celecoxib ( $0.0071 \pm 0.00032 \text{ nmol}/\text{mm}^2$ , mean  $\pm$  SD,  $n = 4$ ).

Since all NSAIDs penetrated slower than transcellular marker diazepam, which is proposed to permeate by passive diffusion, the question arose about the role of transporter proteins for NSAID transport. While NSAIDs are known for their inhibitory activity on cyclo-oxygenase enzymes (COX) affecting prostaglandin synthesis, they have also been described to have a direct inhibitory effect on transporters of prostaglandins. The uptake of prostaglandins is mainly facilitated by organic anion transporters (OATs) [39], while their efflux is regulated by the multidrug resistance protein 4 (MRP4), an ATP-binding cassette (ABC) transporter, associated with multidrug resistance [40]. Ibuprofen was able to inhibit transporter MRP4 (ABCC4) in human embryonic kidney cells (HEK293) at a concentration of  $200 \mu\text{M}$  [40] or in peripheral blood lymphocyte (PBL) cells at a concentration of  $10 \mu\text{M}$ . In the latter case, ibuprofen treatment increased the intracellular levels of the antiretroviral drug zidovudine, whose efflux is facilitated by MRP4 [41]. The inhibitory effects of diclofenac, celecoxib and piroxicam on MRP4 function in HEK203 cells were weaker in comparison to ibuprofen [40,42]. These data confirmed interactions of the investigated NSAIDs with transporter proteins. Thus, we decided to test the influence of inhibitors of multidrug resistance transporters, probenecid and verapamil, on the transport properties of NSAIDs in our model. Probenecid is known to inhibit MRP4 [43] as well as OAT1 or OAT3 [44], while verapamil is a well-known inhibitor of P-glycoprotein (ABCB1) as well as of MRP1 (ABCC1) [45]. Results revealed overall a higher inhibitory effect by

probenecid on NSAID transport than verapamil, increasing the permeability of celecoxib, diclofenac and ibuprofen, whereas an increase upon verapamil was only detected for piroxicam. As the addition of multidrug resistance transporter inhibitors affected the transport of the applied NSAIDs, a concentration-dependent, active transport component could be assumed. The presence of a concentration-dependent permeation behaviour of NSAIDs across cell membranes, especially ibuprofen, has been described in detail previously [46]. A very slight increase in the permeability of paracellular marker CF was detected after probenecid addition, which could be related to publications reporting that CF might be also a moderate substrate for OAT [47] or MRP [48] transporters.

A literature search for *in vivo* or *ex vivo* studies with free NSAID led only to limited results. For example, permeation of piroxicam in combination with various cyclodextrins for better solubility was investigated by Kontogiannidou et al. (2019) *ex vivo* across porcine oral mucosa, who reported an apparent permeability, for instance, for a 1:1 mixture of piroxicam: $\beta$ -cyclodextrin of  $0.21 \pm 0.08 \times 10^{-3}$  cm/h ( $n = 5$ , mean  $\pm$  SD), equivalent to  $0.035 \pm 0.013$   $\mu$ m/min [49]. This permeation coefficient for piroxicam: $\beta$ -cyclodextrin across porcine oral mucosa was over 80 times smaller than the result shown across our *in vitro* model. This could be due to (i) the significantly higher thickness of the porcine mucosa (600–850  $\mu$ m) compared to our cellular model and (ii) the lack of blank studies considering the effects of the tissues' extracellular matrix for the calculation of permeability coefficients in *ex vivo* studies. Moreover, the addition of solubility-enhancing components such as  $\beta$ -cyclodextrin is common for *ex vivo* permeability studies, but should also be considered when comparing these data to the presented *in vitro* results here. In general, testing of whole dosage forms, for instance, often accomplished with *ex vivo* tissues in the Franz Cell system, should also be feasible with our oral mucosa model.

To evaluate if physicochemical properties of the NSAIDs correlate with their calculated permeability coefficient, publicly available data were used for comparison (see Table S3). While XlogP3 values showed no correlation with the permeability coefficient (PC) values, CXlogD at pH 7.4 correlated with the permeability coefficient values with  $R^2 = 0.5797$  ( $R = 0.761$ ). Calculation of CXlogD at pH 7.4 vs. XlogPC led to a higher  $R^2$  value of 0.6649 ( $R = 0.815$ ). Considering the pH value of the experimental set-up improved the correlation, but it should be noted that the found involvement of active transport systems already supported the assumption that lipophilicity and distribution parameters are not sufficient for an accurate prediction of NSAID permeability across the applied oral mucosa *in vitro* model.

Upon determining the transport ranking of celecoxib, diclofenac, ibuprofen and piroxicam and evidence of involvement of multidrug resistance transporters, we aimed to test whether the transport of NSAIDs might change under inflammatory conditions. For this, we chose to investigate the permeability of ibuprofen in combination with probenecid, since literature research showed the highest popularity for ibuprofen and the smallest risk for severe side effects of the mostly prescribed NSAIDs [30–32]. The cultivation conditions of our oral mucosa model were adapted prior to exposure to pro-inflammatory cytokines (TNF- $\alpha$ , IL-1 $\beta$  and IFN- $\gamma$ ) since HKGS, a supplement in cultivation media, contained hydrocortisone, a corticosteroid with anti-inflammatory properties, in particular to IL-1 $\beta$ -induced inflammation response [50]. Hence, cellular layers were washed with media without HKGS 72 h prior to the start of inflammation studies, to reduce the content of hydrocortisone on cell layers, considering its biological half-life of 8–12 h [51]. After these 72 h cultivations without HKGS, cells were treated either with inflammatory cytokines (TNF- $\alpha$ , IL-1 $\beta$  and IFN- $\gamma$ ), ibuprofen, or cytokines plus ibuprofen for 48 h. Ibuprofen was applied at 100  $\mu$ M, a concentration similar to measured plasma concentration (116–142.5  $\mu$ M) after oral administration of 200 mg [52,53]. First, the response of our *in vitro* model on the inflammatory cytokine mixture was evaluated on the mRNA level. Regulation of Janus kinase 1 (JAK1), TNF receptor-associated factor 2 (TRAF2) and RelA was determined. While JAK1 is downstream of the INF- $\gamma$  receptor, involved in signaling of pro-inflammatory cytokines, such as IL-6, IL-7, IL-10 or IL-21, and serves as a therapeutic target in autoimmune diseases, such as

bowel disease [54], TRAF2 mediates the TNF- $\alpha$  mediated response and is essential for the activation of transcription factors, such as the nuclear factor- $\kappa$ Bs (NF $\kappa$ B) [55]. Even though all transcription variants of JAK1 and TRAF2 showed an upregulation upon exposure to cytokines (Figure 2A), no difference was measured in comparison to cells treated with cytokines plus ibuprofen. On the other hand, RelA (also known as p65), a member of the NF- $\kappa$ B family [56] and involved in regulation of NF- $\kappa$ B down the “canonical” pathway [57], was upregulated by cytokine treatment, which was partly blocked by ibuprofen, confirming the anti-inflammatory effects of ibuprofen on this specific pathway.

Since NSAIDs mainly inhibit the activity of COX-1 and COX-2, with the latter increasingly expressed during inflammation, their regulation was analysed on the protein level (Figure 2B). COX-1 was ubiquitously expressed in all treatment groups, while COX-2 was only expressed in cells treated with cytokines, confirming the pro-inflammatory cytokine-dependent upregulation of COX-2. Interestingly, cells treated with cytokines and ibuprofen showed a distinct higher regulation of COX-2 compared to cells treated with cytokines alone. In this regard, it was shown that NSAIDs could display an inhibitory effect on TNF-induced NF- $\kappa$ B activity, and since NF- $\kappa$ B is a key regulator for expression of COX-2, inhibition of NF- $\kappa$ B leads to suppression of COX-2 expression [58]. Besides this, Paik et al. (2000) demonstrated an NF- $\kappa$ B-independent upregulation of COX-2 in human cell lines by an NSAID (flufenamic acid) [59]. Moreover, upregulation of COX-2 was found in prostate cancer cells (PC3 cells) after treatment with 1500  $\mu$ M ibuprofen for 24 h [60] and a recent study by Chai et al. (2015) demonstrated similar findings [61]. However, no up-regulation of COX-2 by ibuprofen was found in our cells without the addition of cytokines, suggesting an induced COX-2 expression boosted by the combination of pro-inflammatory cytokines with ibuprofen after 48 h treatment. In this context, clinical studies reported induced COX-2 expression in the oral mucosa 48 h post-surgery in patients treated with ibuprofen and rofecoxib compared to the placebo group [62]. In addition, higher levels of COX-2 were found after treatment with NSAIDs post-surgery [63].

Next to the increased COX-2 expression levels in the cells of our oral mucosa model after the addition of cytokines, we measured levels of cytokines (IL-1 $\alpha$ , IL-1 $\beta$ , IL-6, IL-8, IFN- $\gamma$ , TNF- $\alpha$ ) and chemokine MCP-1 in the apical and basolateral compartments. After 48 h treatment, levels of added cytokines IL-1 $\beta$ , IFN- $\gamma$  and TNF- $\alpha$  were still distinctly higher in the media of cells which were treated with these cytokines in comparison to cells which did not receive the cytokine mixture. In this regard, it was not possible to define how much the residual amount of non-degraded cytokines contributed to the detected concentration of cytokines. However, concentrations of non-added cytokines IL-1 $\alpha$  and IL-6 and chemokine MCP-1 were also distinctly higher in the media from cells treated with the cytokine mixture, confirming that these cell layers were inflamed and secreted signaling molecules into the media. In general, apical concentrations of cytokines IL-1 $\alpha$  and IL-6 and chemokine MCP-1 were higher than the concentrations found in the basolateral compartment, indicating that the secretion was probably restricted to the blood compartment. For the leveling of these numbers, the different volumes of the apical and basolateral compartments leading to a different dilution factor per cell surface as well as the possible influence of the porous plastic membranal support restricting the access to the basolateral compartment versus free access to the apical fluid should be considered. In accordance with our model set-up and findings, elevated concentration of IFN- $\gamma$  was measured in inflamed oral mucosa tissue in comparison to healthy tissue in a clinical trial [64]. Interestingly, we found very minor regulation of IL-8 in our model. Using the same cell line as we did, cultivated on 24-well plates for one week, Tetyczka et al. (2021) showed an elevated protein level of IL-8 in the supernatants of media after 24 h exposure to IL-1 $\beta$  and TNF- $\alpha$  (100–400 ng/mL) [65]. While IFN- $\gamma$  is described to be involved in inflammatory responses and cell death, a recent study using knock-out mice reported aggravated inflammatory response due to deficiency of IFN- $\gamma$  [66]. Previous studies reported similar results, suggesting anti-inflammatory activities of IFN- $\gamma$  [67,68]. In this regard, it could be speculated that the additionally applied IFN- $\gamma$  in our experiments might be responsible for the absence of regulation of IL-8 in our model.

However, preliminary studies with our model showed no significant disruption of the integrity of the paracellular barrier upon exposure to IL-1 $\beta$  and TNF- $\alpha$  alone, in contrast to our findings shown in Figure 3, suggesting a direct link of IFN- $\gamma$  to the disruption of the paracellular barrier. This was confirmed by previous studies describing a reversible defect on the paracellular barrier of an epithelial intestine model upon exposure to IFN- $\gamma$  [69].

Moreover, media without serum led to lower TEER overall after 48h (Figure 3). A significant reduction was observed for cells treated with cytokines or cytokines with ibuprofen compared to controls, possibly linked to higher permeability of carboxyfluorescein and ibuprofen in those treatment groups. Interestingly, while probenecid was shown to increase the permeability of ibuprofen in controls, similarly to previous transport studies, no tendency of increase was observed in cells treated with cytokines. This indicated a shift of efflux and influx transporters upon treatment with cytokines, either through downregulated efflux systems or possibly through increased inhibition of influx transporters by probenecid. In this regard, 48 h cytokine treatment of our oral mucosa in vitro model led to significant regulation at the mRNA level of transporter and tight junction proteins such as ABCC4 (MRP4), determined by high-throughput qPCR (see Supplementary Table S2). Similarly, previous studies have shown a downregulation of efflux transporter ABCG2 at the mRNA level and a time-dependent (6, 24, 48 h) regulation of protein expression for ABCB1 and ABCG2 upon exposure to IL-1 $\beta$  and TNF alpha at the blood–brain barrier [70]. Characterisation of the used in vitro model based on TR146 cells demonstrated the expression and functionality of those efflux transporters [29]. Hence, future studies should include analysis of the expression of ATP-binding cassettes as well as solute carriers on the protein and functional level at several time points after inflammation to determine the regulatory mechanism of transporters involved upon inflammation stimuli. Additionally, since administration of multidrug resistance transporter inhibitors suggested the presence of active transport systems for the investigated NSAIDs in the TR146 model from the apical to the basolateral compartment, future studies could include transport studies from the basolateral compartment to the apical compartment to analyse a potential polarisation of NSAID transport, as previously detected for C-reactive protein in the TR146 model [24].

## 5. Conclusions

All in all, we applied a model of the oral mucosa epithelium for transport studies with various NSAIDs in combination with inhibitors for active transporter systems, showing distinct substance-dependent differences, with the highest permeability for ibuprofen. Additionally, the buccal mucosa epithelium model showed an inflammatory response after treatment with pro-inflammatory cytokines at the mRNA and protein level and revealed an impaired paracellular barrier linked to IFN- $\gamma$ . Transport studies demonstrated an elevated transport of ibuprofen across inflamed oral mucosa epithelial cells but no increased permeability of ibuprofen with probenecid in contrast to controls, suggesting a shift of transporter systems upon exposure to inflammatory stimuli.

**Supplementary Materials:** The following supporting information can be downloaded at: <https://www.mdpi.com/article/10.3390/pharmaceutics16040543/s1>, Table S1: Overview of PS values (blank, all: cell + blank, cell) and permeability values of cell (PC) and cell + blank (PE) from transport studies with NSAIDs; Table S2: Overview of mRNA expression after inflammation studies analysed with a high-throughput (96.96) qPCR chip; Table S3: Overview of physicochemical properties of NSAIDs, accessed on public databases, and calculated permeability coefficients of NSAIDs in this study. References [29,71] are cited in the supplementary materials.

**Author Contributions:** Conceptualization, G.C.L. and W.N.; methodology, G.C.L., H.-P.F., S.G., A.G. and W.N.; formal analysis, G.C.L. and W.N.; investigation, G.C.L., H.-P.F., S.G. and A.G.; resources, W.N.; writing—original draft preparation, G.C.L.; writing—review and editing, G.C.L. and W.N.; supervision W.N.; project administration, G.C.L. and W.N.; funding acquisition, W.N. All authors have read and agreed to the published version of the manuscript.

**Funding:** This research received no external funding.

**Institutional Review Board Statement:** Not applicable.

**Informed Consent Statement:** Not applicable.

**Data Availability Statement:** The data presented in this study are available on request from the corresponding author.

**Acknowledgments:** Special thanks to Verena Höld (AIT Austrian Institute of Technology GmbH) for her help during the set-up of the first analysis with the HPLC. Open Access Funding by the University of Vienna.

**Conflicts of Interest:** The authors declare no conflicts of interest.

## References

- Hawkey, C.J. COX-2 chronology. *Gut* **2005**, *54*, 1509–1514. [[CrossRef](#)] [[PubMed](#)]
- Vonkeman, H.E.; van de Laar, M.A.F.J. Nonsteroidal Anti-Inflammatory Drugs: Adverse Effects and Their Prevention. *Semin. Arthritis Rheum.* **2010**, *39*, 294–312. [[CrossRef](#)] [[PubMed](#)]
- White, P.F. What are the advantages of non-opioid analgesic techniques in the management of acute and chronic pain? *Expert Opin. Pharmacother.* **2017**, *18*, 329–333. [[CrossRef](#)] [[PubMed](#)]
- Holdgate, A.; Pollock, T. Nonsteroidal anti-inflammatory drugs (NSAIDs) versus opioids for acute renal colic. *Cochrane Database Syst. Rev.* **2004**, CD004137. [[CrossRef](#)]
- Licciardone, J.C.; Gatchel, R.J.; Aryal, S. Effects of Opioids and Nonsteroidal Anti-Inflammatory Drugs on Chronic Low Back Pain and Related Measures: Results from the PRECISION Pain Research Registry. *Tex. Med.* **2018**, *114*, e1. [[PubMed](#)]
- Bhala, N.; Emberson, J.; Merhi, A.; Abramson, S.; Arber, N.; Baron, J.A.; Bombardier, C.; Cannon, C.; Farkouh, M.E.; FitzGerald, G.A.; et al. Vascular and upper gastrointestinal effects of non-steroidal anti-inflammatory drugs: Meta-analyses of individual participant data from randomised trials. *Lancet* **2013**, *382*, 769–779. [[CrossRef](#)] [[PubMed](#)]
- Radi, Z.A.; Khan, N.K. Effects of cyclooxygenase inhibition on the gastrointestinal tract. *Exp. Toxicol. Pathol.* **2006**, *58*, 163–173. [[CrossRef](#)] [[PubMed](#)]
- Gunaydin, C.; Bilge, S.S. Effects of Nonsteroidal Anti-Inflammatory Drugs at the Molecular Level. *Eurasian J. Med.* **2018**, *50*, 116–121. [[CrossRef](#)] [[PubMed](#)]
- Ghlichloo, I.G.V. Nonsteroidal Anti-inflammatory Drugs (NSAIDs). In *StatPearls [Internet]*; StatPearls Publishing: Treasure Island, FL, USA, 2021.
- Meek, I.L.; Van de Laar, M.A.F.J.; Vonkeman, H.E. Non-Steroidal Anti-Inflammatory Drugs: An Overview of Cardiovascular Risks. *Pharmaceuticals* **2010**, *3*, 2146–2162. [[CrossRef](#)]
- Schmid, T.; Brüne, B. Prostanoids and Resolution of Inflammation—Beyond the Lipid-Mediator Class Switch. *Front. Immunol.* **2021**, *12*, 714042. [[CrossRef](#)]
- Brzozowski, T.; Konturek, P.C.; Konturek, S.J.; Sliwowski, Z.; Pajdo, R.; Drozdowicz, D.; Ptak, A.; Hahn, E.G. Classic NSAID and selective cyclooxygenase (COX)-1 and COX-2 inhibitors in healing of chronic gastric ulcers. *Microsc. Res. Tech.* **2001**, *53*, 343–353. [[CrossRef](#)]
- Kowalski, M.L.; Makowska, J.S. Seven steps to the diagnosis of NSAIDs hypersensitivity: How to apply a new classification in real practice? *Allergy Asthma Immunol. Res.* **2015**, *7*, 312–320. [[CrossRef](#)] [[PubMed](#)]
- Blanca-Lopez, N.; Soriano, V.; Garcia-Martin, E.; Canto, G.; Blanca, M. NSAID-induced reactions: Classification, prevalence, impact, and management strategies. *J. Asthma Allergy* **2019**, *12*, 217–233. [[CrossRef](#)] [[PubMed](#)]
- Chandrasekharan, N.V.; Dai, H.; Roos, K.L.T.; Evanson, N.K.; Tomsik, J.; Elton, T.S.; Simmons, D.L. COX-3, a cyclooxygenase-1 variant inhibited by acetaminophen and other analgesic/antipyretic drugs: Cloning, structure, and expression. *Proc. Natl. Acad. Sci. USA* **2002**, *99*, 13926–13931. [[CrossRef](#)] [[PubMed](#)]
- Brogan, S.E.; Mandyam, S.; Odell, D.W. 19—Nonopioid Analgesics. In *Pharmacology and Physiology for Anesthesia*, 2nd ed.; Hemmings, H.C., Egan, T.D., Eds.; Elsevier: Philadelphia, PA, USA, 2019; pp. 369–389. ISBN 978-0-323-48110-6. [[CrossRef](#)]
- Wright, S.; Yelland, M.; Heathcote, K.; Ng, S.-K.; Wright, G. Fear of needles—Nature and prevalence in general practice. *Aust. Fam. Physician* **2009**, *38*, 172–176.
- McLenon, J.; Rogers, M.A.M. The fear of needles: A systematic review and meta-analysis. *J. Adv. Nurs.* **2019**, *75*, 30–42. [[CrossRef](#)]
- Hua, S. Advances in nanoparticulate drug delivery approaches for sublingual and buccal administration. *Front. Pharmacol.* **2019**, *10*, 491535. [[CrossRef](#)]
- Sun, B.; Wang, W.; He, Z.; Zhang, M.; Kong, F.; Sain, M. Biopolymer Substrates in Buccal Drug Delivery: Current Status and Future Trend. *Curr. Med. Chem.* **2020**, *27*, 1661–1669. [[CrossRef](#)] [[PubMed](#)]
- Nazari, K.; Kontogiannidou, E.; Ahmad, R.H.; Gratsani, A.; Rasekh, M.; Arshad, M.S.; Sunar, B.S.; Armitage, D.; Bouropoulos, N.; Chang, M.W.; et al. Development and characterisation of cellulose based electrospun mats for buccal delivery of non-steroidal anti-inflammatory drug (NSAID). *Eur. J. Pharm. Sci.* **2017**, *102*, 147–155. [[CrossRef](#)]
- Marques, A.C.; Rocha, A.I.; Leal, P.; Estanqueiro, M.; Lobo, J.M.S. Development and characterization of mucoadhesive buccal gels containing lipid nanoparticles of ibuprofen. *Int. J. Pharm.* **2017**, *533*, 455–462. [[CrossRef](#)]
- Smart, J.D. Buccal drug delivery. *Expert Opin. Drug Deliv.* **2005**, *2*, 507–517. [[CrossRef](#)]

24. Lin, G.C.; Küng, E.; Smajlhodzic, M.; Domazet, S.; Friedl, H.P.; Angerer, J.; Wisgrill, L.; Berger, A.; Bingle, L.; Peham, J.R.; et al. Directed Transport of CRP Across In Vitro Models of the Blood-Saliva Barrier Strengthens the Feasibility of Salivary CRP as Biomarker for Neonatal Sepsis. *Pharmaceutics* **2021**, *13*, 256. [[CrossRef](#)] [[PubMed](#)]
25. Lin, G.C.; Smajlhodzic, M.; Bandian, A.-M.; Friedl, H.-P.; Leitgeb, T.; Oerter, S.; Stadler, K.; Giese, U.; Peham, J.R.; Bingle, L.; et al. An In Vitro Barrier Model of the Human Submandibular Salivary Gland Epithelium Based on a Single Cell Clone of Cell Line HTB-41: Establishment and Application for Biomarker Transport Studies. *Biomedicines* **2020**, *8*, 302. [[CrossRef](#)] [[PubMed](#)]
26. Day, R.; Geisslinger, G.; Paull, P.; Williams, K. Neither cimetidine nor probenecid affect the pharmacokinetics of tenoxicam in normal volunteers. *Br. J. Clin. Pharmacol.* **1994**, *37*, 79–81. [[CrossRef](#)] [[PubMed](#)]
27. Al-Tuwaijri, A.S.; Mustafa, A.A. Verapamil enhances the inhibitory effect of diclofenac on the chemiluminescence of human polymorphonuclear leukocytes and carrageenan-induced rat's paw oedema. *Int. J. Immunopharmacol.* **1992**, *14*, 83–91. [[CrossRef](#)]
28. Dong, P.-L.; Han, H.; Zhang, T.-Y.; Yang, B.; Wang, Q.-H.; Eerdun, G.-W. P-glycoprotein inhibition increases the transport of dauricine across the blood-brain barrier. *Mol. Med. Rep.* **2014**, *9*, 985–988. [[CrossRef](#)] [[PubMed](#)]
29. Lin, G.C.; Leitgeb, T.; Vladetic, A.; Friedl, H.-P.; Rhodes, N.; Rossi, A.; Roblegg, E.; Neuhaus, W. Optimization of an oral mucosa in vitro model based on cell line TR146. *Tissue Barriers* **2020**, *8*, 1748459. [[CrossRef](#)]
30. Valkhoff, V.E.; Schade, R.; 't Jong, G.W.; Romio, S.; Schuemie, M.J.; Arfe, A.; Garbe, E.; Herings, R.; Lucchi, S.; Picelli, G.; et al. Population-based analysis of non-steroidal anti-inflammatory drug use among children in four European countries in the SOS project: What size of data platforms and which study designs do we need to assess safety issues? *BMC Pediatr.* **2013**, *13*, 192. [[CrossRef](#)] [[PubMed](#)]
31. McGettigan, P.; Henry, D. Use of Non-Steroidal Anti-Inflammatory Drugs That Elevate Cardiovascular Risk: An Examination of Sales and Essential Medicines Lists in Low-, Middle-, and High-Income Countries. *PLoS Med.* **2013**, *10*, e1001388. [[CrossRef](#)]
32. García-Poza, P.; de Abajo, F.J.; Gil, M.J.; Chacón, A.; Bryant, V.; García-Rodríguez, L.A. Risk of ischemic stroke associated with non-steroidal anti-inflammatory drugs and paracetamol: A population-based case-control study. *J. Thromb. Haemost.* **2015**, *13*, 708–718. [[CrossRef](#)]
33. Novakova, I.; Subileau, E.A.; Toegel, S.; Gruber, D.; Lachmann, B.; Urban, E.; Chesne, C.; Noe, C.R.; Neuhaus, W. Transport rankings of non-steroidal antiinflammatory drugs across blood-brain barrier in vitro models. *PLoS ONE* **2014**, *9*, e86806. [[CrossRef](#)]
34. Rohani Shirvan, A.; Hemmatinejad, N.; Bahrami, S.H.; Bashari, A. Fabrication of multifunctional mucoadhesive buccal patch for drug delivery applications. *J. Biomed. Mater. Res. A* **2021**, *109*, 2640–2656. [[CrossRef](#)] [[PubMed](#)]
35. Eleftheriadis, G.K.; Katsiotis, C.S.; Andreadis, D.A.; Tzetzis, D.; Ritzoulis, C.; Bouropoulos, N.; Kanellopoulou, D.; Andriotis, E.G.; Tsibouklis, J.; Fatouros, D.G. Inkjet printing of a thermolabile model drug onto FDM-printed substrates: Formulation and evaluation. *Drug Dev. Ind. Pharm.* **2020**, *46*, 1253–1264. [[CrossRef](#)] [[PubMed](#)]
36. Usansky, H.H.; Sinko, P.J. Estimating human drug oral absorption kinetics from Caco-2 permeability using an absorption-disposition model: Model development and evaluation and derivation of analytical solutions for  $k_a$  and  $F_a$ . *J. Pharmacol. Exp. Ther.* **2005**, *314*, 391–399. [[CrossRef](#)] [[PubMed](#)]
37. Wang, T.; Zhao, P.; Zhao, Q.; Wang, B.; Wang, S. The mechanism for increasing the oral bioavailability of poorly water-soluble drugs using uniform mesoporous carbon spheres as a carrier. *Drug Deliv.* **2016**, *23*, 420–428. [[CrossRef](#)]
38. Lee, J.B.; Zgair, A.; Taha, D.A.; Zang, X.; Kagan, L.; Kim, T.H.; Kim, M.G.; Yun, H.y.; Fischer, P.M.; Gershkovich, P. Quantitative analysis of lab-to-lab variability in Caco-2 permeability assays. *Eur. J. Pharm. Biopharm.* **2017**, *114*, 38–42. [[CrossRef](#)] [[PubMed](#)]
39. Kimura, H.; Takeda, M.; Narikawa, S.; Enomoto, A.; Ichida, K.; Endou, H. Human organic anion transporters and human organic cation transporters mediate renal transport of prostaglandins. *J. Pharmacol. Exp. Ther.* **2002**, *301*, 293–298. [[CrossRef](#)]
40. Reid, G.; Wielinga, P.; Zelcer, N.; Van der Heijden, I.; Kuil, A.; De Haas, M.; Wijnholds, J.; Borst, P. The human multidrug resistance protein MRP4 functions as a prostaglandin efflux transporter and is inhibited by nonsteroidal anti inflammatory drugs. *Proc. Natl. Acad. Sci. USA* **2003**, *100*, 9244–9249. [[CrossRef](#)]
41. Clemente, M.I.; Álvarez, S.; Serramía, M.J.; Turriziani, O.; Genebat, M.; Leal, M.; Fresno, M.; Muñoz-Fernández, M.A. Non-steroidal anti-inflammatory drugs increase the antiretroviral activity of nucleoside reverse transcriptase inhibitors in HIV type-1-infected T-lymphocytes: Role of multidrug resistance protein 4. *Antivir. Ther.* **2009**, *14*, 1101–1111. [[CrossRef](#)]
42. El-Sheikh, A.A.K.; Van Den Heuvel, J.J.M.W.; Koenderink, J.B.; Russel, F.G.M. Interaction of nonsteroidal anti-inflammatory drugs with multidrug resistance protein (MRP) 2/ABCC2- and MRP4/ABCC4-mediated methotrexate transport. *J. Pharmacol. Exp. Ther.* **2007**, *320*, 229–235. [[CrossRef](#)]
43. Russel, F.G.M.; Koenderink, J.B.; Masereeuw, R. Multidrug resistance protein 4 (MRP4/ABCC4): A versatile efflux transporter for drugs and signalling molecules. *Trends Pharmacol. Sci.* **2008**, *29*, 200–207. [[CrossRef](#)] [[PubMed](#)]
44. Hagos, F.T.; Daood, M.J.; Ocque, J.A.; Nolin, T.D.; Bayir, H.; Poloyac, S.M.; Kochanek, P.M.; Clark, R.S.B.; Empey, P.E. Probenecid, an organic anion transporter 1 and 3 inhibitor, increases plasma and brain exposure of N-acetylcysteine. *Xenobiotica* **2017**, *47*, 346–353. [[CrossRef](#)] [[PubMed](#)]
45. Perrotton, T.; Trompier, D.; Chang, X.-B.; Di Pietro, A.; Baubichon-Cortay, H. (R)- and (S)-Verapamil Differentially Modulate the Multidrug-resistant Protein MRP1. *J. Biol. Chem.* **2007**, *282*, 31542–31548. [[CrossRef](#)] [[PubMed](#)]

46. Ghorbani, M.; Dehghan, G.; Allahverdi, A. Concentration-dependent mechanism of the binding behavior of ibuprofen to the cell membrane: A molecular dynamic simulation study. *J. Mol. Graph. Model.* **2023**, *124*, 108581. [[CrossRef](#)] [[PubMed](#)]
47. Truong, D.M.; Kaler, G.; Khandelwal, A.; Swaan, P.W.; Nigam, S.K. Multi-level analysis of organic anion transporters 1, 3, and 6 reveals major differences in structural determinants of antiviral discrimination. *J. Biol. Chem.* **2008**, *283*, 8654–8663. [[CrossRef](#)] [[PubMed](#)]
48. Lee, G.; Piquette-Miller, M. Cytokines alter the expression and activity of the multidrug resistance transporters in human hepatoma cell lines; analysis using RT-PCR and cDNA microarrays. *J. Pharm. Sci.* **2003**, *92*, 2152–2163. [[CrossRef](#)] [[PubMed](#)]
49. Kontogiannidou, E.; Ferrari, M.; Deligianni, A.D.; Bouropoulos, N.; Andreadis, D.A.; Sorrenti, M.; Catenacci, L.; Nazari, K.; Arshad, M.S.; Chang, M.W.; et al. In Vitro and Ex Vivo Evaluation of Tablets Containing Piroxicam-Cyclodextrin Complexes for Buccal delivery. *Pharmaceutics* **2019**, *11*, 398. [[CrossRef](#)] [[PubMed](#)]
50. Rautava, S.; Walker, W.A.; Lu, L. Hydrocortisone-induced anti-inflammatory effects in immature human enterocytes depend on the timing of exposure. *Am. J. Physiol. Gastrointest. Liver Physiol.* **2016**, *310*, G920–G929. [[CrossRef](#)]
51. Cevc, G.; Blume, G. Hydrocortisone and dexamethasone in very deformable drug carriers have increased biological potency, prolonged effect, and reduced therapeutic dosage. *Biochim. Biophys. Acta (BBA) Biomembr.* **2004**, *1663*, 61–73. [[CrossRef](#)]
52. Sugár, D.; Francombe, D.; da Silva, T.; Hanid, S.; Hutchings, S. Comparative Bioavailability Study of a New Orodispersible Formulation of Ibuprofen Versus Two Existing Oral Tablet Formulations in Healthy Male and Female Volunteers. *Clin. Ther.* **2019**, *41*, 1486–1498. [[CrossRef](#)]
53. Shin, D.; Lee, S.J.; Ha, Y.-M.; Choi, Y.-S.; Kim, J.-W.; Park, S.-R.; Park, M.K. Pharmacokinetic and pharmacodynamic evaluation according to absorption differences in three formulations of ibuprofen. *Drug Des. Dev. Ther.* **2017**, *11*, 135–141. [[CrossRef](#)] [[PubMed](#)]
54. Spinelli, F.R.; Colbert, R.A.; Gadina, M. JAK1: Number one in the family; Number one in inflammation? *Rheumatology* **2021**, *60*, II3–II10. [[CrossRef](#)] [[PubMed](#)]
55. Lalani, A.I.; Zhu, S.; Gokhale, S.; Jin, J.; Xie, P. TRAF molecules in inflammation and inflammatory diseases. *Curr. Pharmacol. Rep.* **2018**, *4*, 64–90. [[CrossRef](#)] [[PubMed](#)]
56. Bijli, K.M.; Fazal, F.; Rahman, A. Regulation of RelA/p65 and endothelial cell inflammation by proline-rich tyrosine kinase 2. *Am. J. Respir. Cell Mol. Biol.* **2012**, *47*, 660–668. [[CrossRef](#)] [[PubMed](#)]
57. Shi, G.; Li, D.; Fu, J.; Sun, Y.; Li, Y.; Qu, R.; Jin, X.; Li, D. Upregulation of cyclooxygenase-2 is associated with activation of the alternative nuclear factor kappa B signaling pathway in colonic adenocarcinoma. *Am. J. Transl. Res.* **2015**, *7*, 1612–1620. [[PubMed](#)]
58. Takada, Y.; Bhardwaj, A.; Potdar, P.; Aggarwal, B.B. Nonsteroidal anti-inflammatory agents differ in their ability to suppress NF- $\kappa$ B activation, inhibition of expression of cyclooxygenase-2 and cyclin D1, and abrogation of tumor cell proliferation. *Oncogene* **2004**, *23*, 9247–9258. [[CrossRef](#)] [[PubMed](#)]
59. Paik, J.H.; Ju, J.H.; Lee, J.Y.; Boudreau, M.D.; Hwang, D.H. Two opposing effects of non-steroidal anti-inflammatory drugs on the expression of the inducible cyclooxygenase: Mediation through different signaling pathways. *J. Biol. Chem.* **2000**, *275*, 28173–28179. [[CrossRef](#)] [[PubMed](#)]
60. John-Aryankalayil, M.; Palayoor, S.T.; Cerna, D.; Falduto, M.T.; Magnuson, S.R.; Coleman, C.N. NS-398, ibuprofen, and cyclooxygenase-2 RNA interference produce significantly different gene expression profiles in prostate cancer cells. *Mol. Cancer Ther.* **2009**, *8*, 261–273. [[CrossRef](#)] [[PubMed](#)]
61. Chai, A.C.; Robinson, A.L.; Chai, K.X.; Chen, L.-M. Ibuprofen regulates the expression and function of membrane-associated serine proteases prostasin and matriptase. *BMC Cancer* **2015**, *15*, 1025. [[CrossRef](#)]
62. Lee, Y.-S.; Kim, H.; Wu, T.-X.; Wang, X.-M.; Dionne, R.A. Genetically mediated interindividual variation in analgesic responses to cyclooxygenase inhibitory drugs. *Clin. Pharmacol. Ther.* **2006**, *79*, 407–418. [[CrossRef](#)]
63. Wang, X.-M.; Wu, T.-X.; Hamza, M.; Ramsay, E.S.; Wahl, S.M.; Dionne, R.A. Rofecoxib modulates multiple gene expression pathways in a clinical model of acute inflammatory pain. *Pain* **2007**, *128*, 136–147. [[CrossRef](#)] [[PubMed](#)]
64. Buño, I.J.; Huff, J.C.; Weston, W.L.; Cook, D.T.; Brice, S.L. Elevated levels of interferon gamma, tumor necrosis factor alpha, interleukins 2, 4, and 5, but not interleukin 10, are present in recurrent aphthous stomatitis. *Arch. Dermatol.* **1998**, *134*, 827–831. [[CrossRef](#)] [[PubMed](#)]
65. Tetyczka, C.; Hartl, S.; Jeitler, R.; Absenger-Novak, M.; Meindl, C.; Fröhlich, E.; Riedl, S.; Zwegtick, D.; Roblegg, E. Cytokine-mediated inflammation in the oral cavity and its effect on lipid nanocarriers. *Nanomaterials* **2021**, *11*, 1330. [[CrossRef](#)] [[PubMed](#)]
66. Lee, S.H.; Kwon, J.y.; Kim, S.-Y.; Jung, K.; Cho, M.-L. Interferon-gamma regulates inflammatory cell death by targeting necroptosis in experimental autoimmune arthritis. *Sci. Rep.* **2017**, *7*, 10133. [[CrossRef](#)] [[PubMed](#)]
67. Jones, L.S.; Rizzo, L.V.; Agarwal, R.K.; Tarrant, T.K.; Chan, C.C.; Wiggert, B.; Caspi, R.R. IFN- $\gamma$ -deficient mice develop experimental autoimmune uveitis in the context of a deviant effector response. *J. Immunol.* **1997**, *158*, 5997–6005. [[CrossRef](#)]
68. Ferber, I.A.; Brocke, S.; Taylor-Edwards, C.; Ridgway, W.; Dinisco, C.; Steinman, L.; Dalton, D.; Fathman, C.G. Mice with a disrupted IFN- $\gamma$  gene are susceptible to the induction of experimental autoimmune encephalomyelitis (EAE). *J. Immunol.* **1996**, *156*, 5–7. [[CrossRef](#)] [[PubMed](#)]
69. Adams, R.B.; Planchon, S.M.; Roche, J.K. IFN- $\gamma$  modulation of epithelial barrier function. Time course, reversibility, and site of cytokine binding. *J. Immunol.* **1993**, *150*, 2356–2363. [[CrossRef](#)] [[PubMed](#)]

- 
70. Von Wedel-Parlow, M.; Wölte, P.; Galla, H.J. Regulation of major efflux transporters under inflammatory conditions at the blood-brain barrier in vitro. *J. Neurochem.* **2009**, *111*, 111–118. [[CrossRef](#)]
  71. Mineta, K.; Yamamoto, Y.; Yamazaki, Y.; Tanaka, H.; Tada, Y.; Saito, K.; Tamura, A.; Igarashi, M.; Endo, T.; Takeuchi, K.; et al. Predicted expansion of the claudin multigene family. *FEBS Lett.* **2011**, *585*, 606–612. [[CrossRef](#)]

**Disclaimer/Publisher’s Note:** The statements, opinions and data contained in all publications are solely those of the individual author(s) and contributor(s) and not of MDPI and/or the editor(s). MDPI and/or the editor(s) disclaim responsibility for any injury to people or property resulting from any ideas, methods, instructions or products referred to in the content.